L. Ojha, M. B. Wilhelm, S. L. Murchie, A. S. McEwen, J. J. Wray, J. Hanley, M. Masse, and M. Chojnacki, "Spectral evidence for hydrated salts in recurring slope lineae on Mars", *Nature Geoscience,* **8**, 829-832 (2015).

1. Mars has an atmospheric pressure of roughly 0.006 atm. Use Figure 11.40 (a) from your text (shown below) to discuss whether flowing water at temperatures of 250-300K is likely to be "pure." Back up your arguments with scientific reasoning.

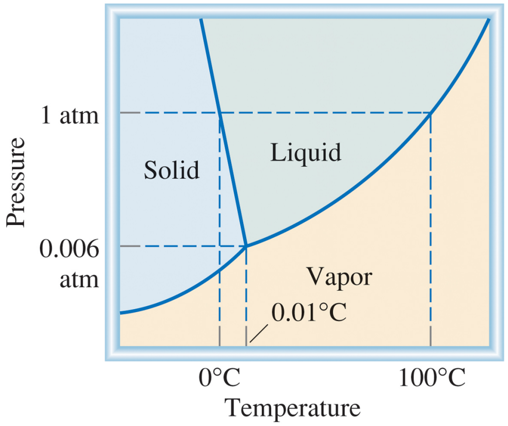

2. The authors suggest that chlorate and perchlorate salts (e.g., sodium perchlorate, magnesium chlorate) provided the best match to spectra associated with the Horowitz crater. Why does the presence of these salts support the possibility of flowing liquid water at these temperatures and pressures? Use the phase diagram of water, and back up your arguments with scientific reasoning.

3. Use your knowledge of colligative properties to justify the claim made by the authors: "Sodium perchlorate can lower the freezing point of water by up to 40 K, whereas magnesium perchlorate and magnesium chlorate can depress the freezing point by up to 70K."

4. Did the scientists definitively identify flowing water on Mars?

5. This data was taken from the Mars Orbiter which, like its name suggests, is in orbit around Mars. Other surface space missions, whether manned or unmanned, have to be extremely careful to not contaminate the environments that are being studied. Suggest possible implications that might result from a lack of planning and foresight in this area; what effect might it have on the analysis of these celestial bodies?

6. What are the possible implications of discovering liquid water on Mars?

nature geoscience

LETTERS

| DOI: 10.1038/NGEO2546

Spectral evidence for hydrated salts in recurring slope lineae on Mars

Lujendra Ojha[1]*, Mary Beth Wilhelm[1,2], Scott L. Murchie[3], Alfred S. McEwen[4], James J. Wray[1], Jennifer Hanley[5], Marion Massé[6] and Matt Chojnacki[4]

Determining whether liquid water exists on the Martian surface is central to understanding the hydrologic cycle and potential for extant life on Mars. Recurring slope lineae, narrow streaks of low reflectance compared to the surrounding terrain, appear and grow incrementally in the downslope direction during warm seasons when temperatures reach about 250–300 K, a pattern consistent with the transient flow of a volatile species[1–3]. Brine flows (or seeps) have been proposed to explain the formation of recurring slope lineae[1–3], yet no direct evidence for either liquid water or hydrated salts has been found[4]. Here we analyse spectral data from the Compact Reconnaissance Imaging Spectrometer for Mars instrument onboard the Mars Reconnaissance Orbiter from four different locations where recurring slope lineae are present. We find evidence for hydrated salts at all four locations in the seasons when recurring slope lineae are most extensive, which suggests that the source of hydration is recurring slope lineae activity. The hydrated salts most consistent with the spectral absorption features we detect are magnesium perchlorate, magnesium chlorate and sodium perchlorate. Our findings strongly support the hypothesis that recurring slope lineae form as a result of contemporary water activity on Mars.

Water is essential to life as we know it. The presence of liquid water on Mars today has astrobiological, geologic and hydrologic implications and may affect future human exploration. Various salts (for example, sulphates, chlorides and perchlorates) have been detected on the surface of Mars from remote and *in situ* investigations[5–7]. These salts can lower the freezing point of water by up to 80 K, lower the evaporation rate of water by an order of magnitude, and can be hygroscopic (that is, able to easily absorb atmospheric moisture), for example, see refs 8–11, thus increasing the possibility of forming and stabilizing liquid water on the surface of present-day Mars[12].

Recurring slope lineae (RSL) are narrow, low-reflectance features forming on present-day Mars that have been suggested to be due to the transient flow of liquid water. RSL extend incrementally downslope on steep, warm slopes, fade when inactive, and reappear annually over multiple Mars years[1–3]. Average RSL range in width from a few metres (<5 m), down to the detection limit for the High Resolution Imaging Science Experiment (HiRISE) camera (~0.25 m pixel^{-1}; ref. 13). The temperatures on slopes where RSL are active typically exceed 250 K and commonly are above 273 K (ref. 2). These characteristics suggest a possible role of salts in lowering the freezing point of water, allowing briny solutions to flow[1–3]. Confirmation of this wet origin hypothesis for RSL would require either detection of liquid water absorptions on the surface, or detection of hydrated salts precipitated from that water.

The mineralogic composition of RSL and their surroundings can be investigated using orbital data acquired by the Compact Reconnaissance Imaging Spectrometer for Mars (CRISM) on the Mars Reconnaissance Orbiter (MRO), which acquires spectral cubes with 544 spectral channels (~0.4 to 3.92 μm; ref. 14). Within the infrared (IR) detector spectral range of CRISM (1–3.92 μm), both liquid water and hydrated salts have diagnostic absorption bands at ~1.4 μm, ~1.9 μm and a broad absorption feature at ~3.0 μm (ref. 15; Fig. 1). In addition, hydrated salts may exhibit combinations or overtones at other wavelengths from 1.7 to 2.4 μm. Given the coarser spatial sampling of CRISM (~18 m pixel^{-1}) compared to HiRISE, few locations exist in which RSL are wide or dense enough to fill even a single CRISM pixel. In this work, we devised a variety of methods to reduce uncertainties from extraction of CRISM spectra from individual pixels (Supplementary Information), allowing examination of pixels mostly filled by RSL.

At Palikir crater, RSL are observed to be longest and widest towards the end of the southern summer. In the HiRISE image acquired at the end of the southern summer of Mars Year (MY) 30, wide RSL were observed on the slopes of Palikir (Fig. 1 and Supplementary Table 1). CRISM spectra from this dense region of RSL were inspected. Six individual CRISM pixels exhibit enhanced hydration absorption features (Fig. 1 and Supplementary Table 1). The CRISM pixels closest to the wide RSL exhibited absorption features at wavelengths near ~1.48, 1.91 (Fig. 1) and ~3 μm (Supplementary Fig. 1), whereas pixels farther away from RSL exhibited absorption features only at ~1.91 and ~3 μm (Supplementary Fig. 1 and Supplementary Table 1). In general, the ~1.4 μm absorption feature generally weakens with dehydration and disappears more rapidly than the ~1.9 and 3 μm absorption bands (for example, see ref. 16). This suggests a higher hydration state in areas closest to the RSL core. The 1.9 μm absorption is also present in the unratioed I/F spectrum, precluding ratio artefacts as the source of the absorption band (Supplementary Fig. 1). We carried out a statistical study to elucidate true signal from noise. The 1.9 μm absorption is consistently well above the noise threshold, and in half of the cases the 1.4 and 2.15 μm absorption features are also above the noise threshold (Supplementary Fig. 2). The wavelength position of the observed 1.4 μm absorption is longer than is typical of perchlorates, suggesting the presence of an additional mineral.

We also analysed CRISM observation of Palikir crater during the middle of MY 30 southern summer, when RSL were shorter and narrower, and found no evidence for absorption features at ~1.4 and/or 1.9 μm anywhere surrounding the RSL (Supplementary Fig. 3

---

[1]School of Earth and Atmospheric Sciences, Georgia Institute of Technology, Atlanta, Georgia 30308, USA. [2]Space Science and Astrobiology Division, NASA Ames Research Center, Moffett Field, California 94035, USA. [3]Applied Physics Laboratory, Laurel, Maryland 20723, USA. [4]Lunar and Planetary Laboratory, University of Arizona, Tucson, Arizona 85721, USA. [5]Department of Space Studies, Southwest Research Institute, Boulder, Colorado 80302, USA. [6]Laboratoire de Planétologie et Géodynamique, Nantes 44322, France. *e-mail: luju@gatech.edu

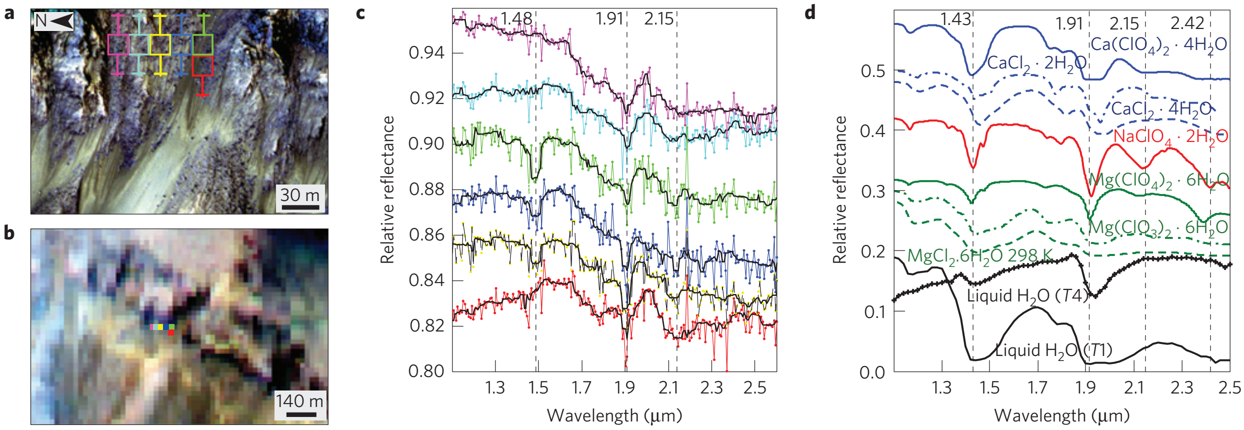

Figure 1 | Palikir crater RSL and spectral detection of hydration features. **a**, RSL on slope of Palikir crater ESP_024034_1380 (Infrared–Red–Blue/Green (IRB)) (L_S: 359 MY: 30). Coloured boxes show the location of the CRISM pixels with the uncertainty. **b**, Concurrent CRISM observation FRT0002038F (R: 2.53 μm, G: 1.51 μm, B: 1.08 μm) showing the same area as **a**. **c**, Spectra from coloured regions of interest shown in **a** and **b**. The observed data are plotted with coloured lines and the smoothed data in black lines. **d**, Laboratory spectra of various salts[17,28,29] and liquid water ($T1 = 1$ and $T4 = 4$ h into dehydration)[16].

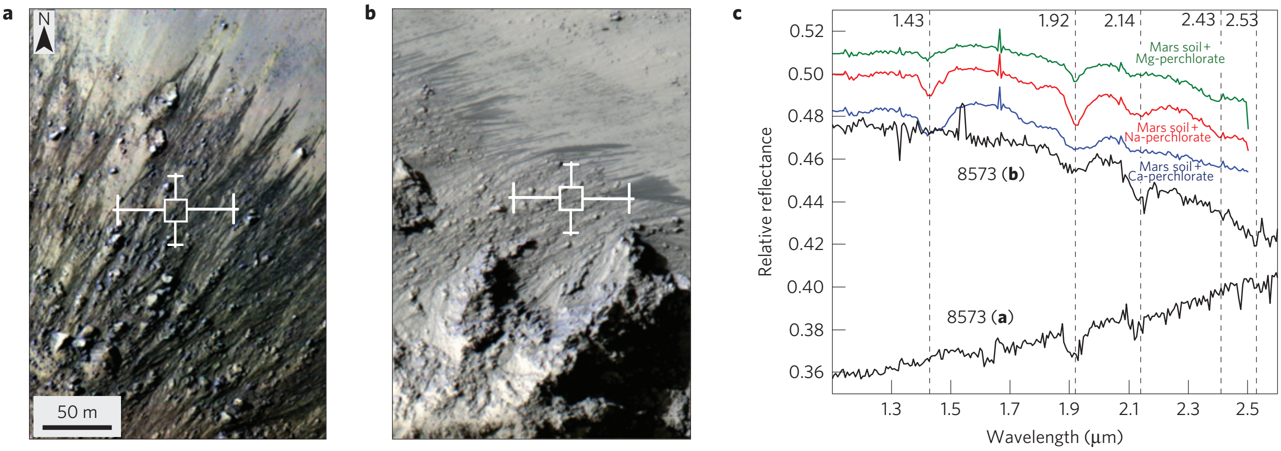

Figure 2 | RSL activity in the central peaks of Horowitz crater and associated CRISM spectra. **a**, RSL emanating from bedrock exposures at Horowitz crater's central peak. Part of HiRISE image PSP_005787_1475 (IRB) ($L_S = 334°$, MY 28). **b**, A different section of the same HiRISE image as **a**, showing RSL activity at a different peak (scale same as in **a**). In **a** and **b**, the white box with error bars shows the location of the CRISM pixels with the uncertainty. **c**, Black spectra correspond to the area in **a** and **b**, from CRISM observation FRT00008573. Coloured spectra are results from spectral mixing between the Martian soil and a variety of salts (specified in the figure).

and Supplementary Table 1). In MY 31, only the image from the end of the summer (FRT00029F0C) showed 1.9 and 3 μm absorptions (Supplementary Fig. 4). Detections of hydration bands from both MY are only from late-season images where RSL are observed to be the widest, consistent with our hypothesis that the hydration feature is due to the areally extensive presence of RSL.

The absorptions observed in CRISM images of Palikir are too narrow to be explained by liquid water. Instead, they may be consistent with hydrated salts (Fig. 1). The rapid change in hydration state of the minerals imply that at the times and places where RSL form, either the hydration state of the minerals is being increased by the presence of RSL, or hydrated minerals are deposited by RSL and later desiccated. A linear spectral mixture of Martian soil with magnesium perchlorate, chlorate and chloride provides the closest match (Supplementary Fig. 5).

Coordinated HiRISE–CRISM observations of Horowitz crater in MY 29 show large RSL emanating from the central peaks (Fig. 2). At two of the central peaks, we observed absorptions at 1.9, 2.15 and 2.43 μm. A linear spectral mixture of Martian soil and sodium perchlorate[17,18] provided the best match to the observed spectra (Fig. 2 and Supplementary Fig. 7). The spectra reported here lack absorption features above the noise threshold at ~1.4 μm, but they do have broad ~3 μm absorptions consistent with hydration (Supplementary Fig. 8). The 1.9 and 2.15 μm absorptions are also present in the unratioed I/F spectrum (Supplementary Fig. 8).

Some of the most intense RSL activity in the southern mid-latitudes occurs on the central peak structures of Hale crater (Fig. 3). A HiRISE–CRISM coordinated observation was acquired during the late RSL season (Fig. 3 and Supplementary Table 1). Analysis of the CRISM data shows strong ~1.48 and 1.9 μm absorption features in the location where dense RSL activity is observed in the HiRISE image (Fig. 3). Similar to Palikir, the presence of narrow 1.48 and 1.9 μm absorption bands is consistent with a linear spectral mixture of magnesium perchlorate and Martian soil.

In Coprates Chasma, RSL are abundant and in some cases entire fans associated with RSL are observed to change their reflectance[2] (Fig. 4). Spectra of RSL fans in Coprates Chasma were analysed, and we found multiple places in the CRISM images with 1.9 μm absorptions (Fig. 4). Without detection of other absorptions, assignment to a particular salt mineralogy is not possible. The 1.9 μm absorption on the RSL slope suggests precipitation of salts and resulting modification of grain sizes as a viable mechanism

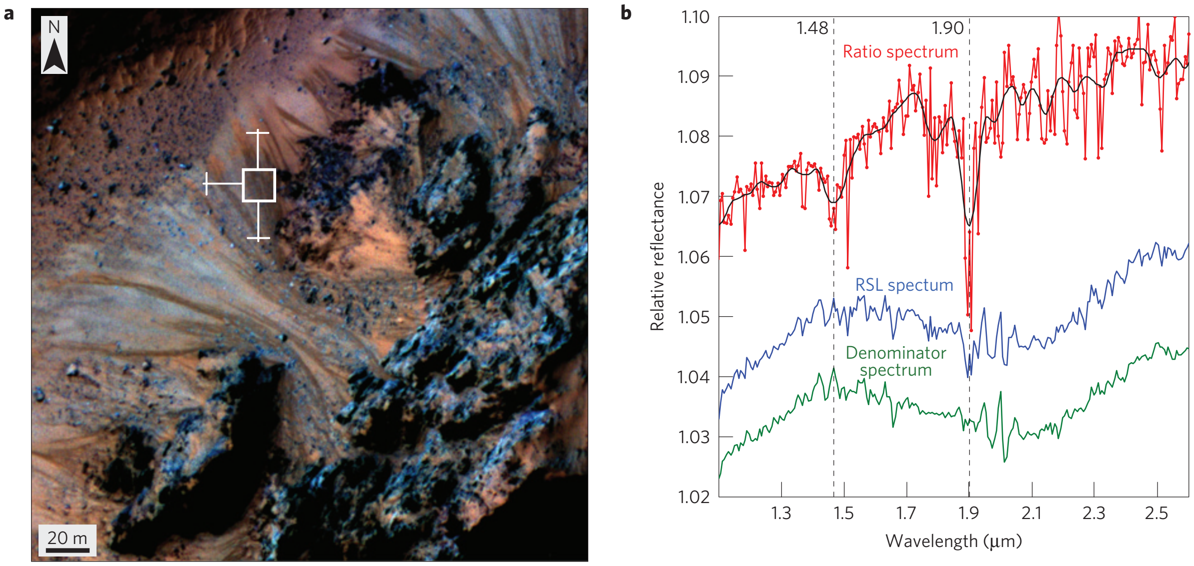

Figure 3 | RSL emanating from a central peak in Hale crater and associated CRISM spectrum. a, RSL on a central peak of Hale crater. Section of HiRISE image ESP_032416_1440 (IRB) ($L_S = 342$, MY 31): north is up and light is from the left. White box with error bars shows the location of the CRISM pixels with the uncertainty. **b**, IR spectrum from the RSL seen in the HiRISE image. The symbols and the smoothing functions used are the same as in Figs 1 and 2.

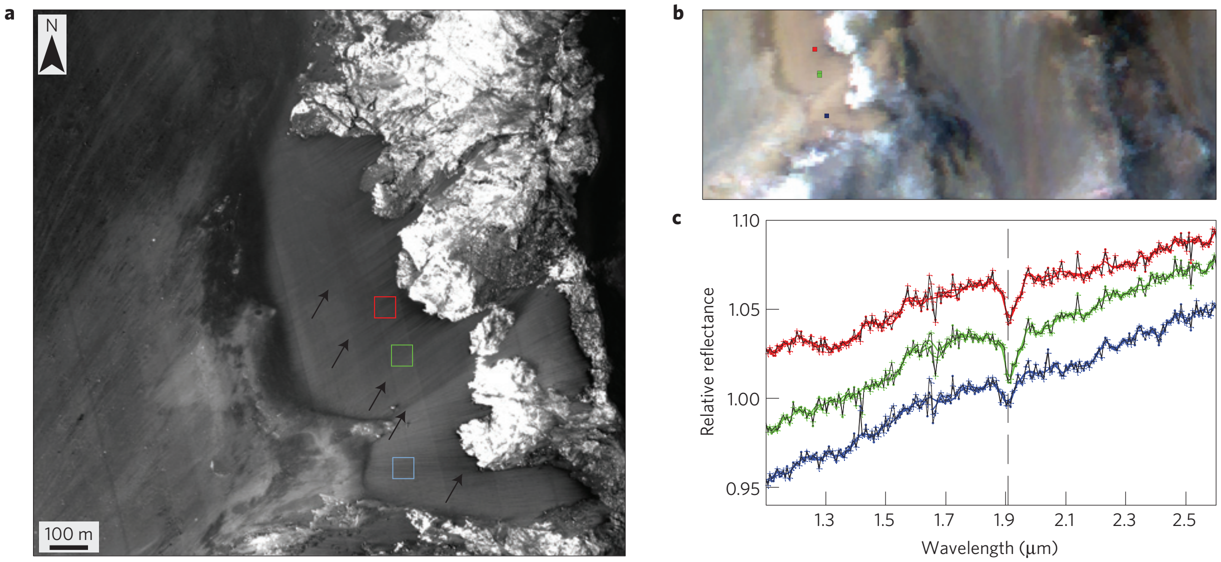

Figure 4 | RSL and associated dark fans observed in Coprates Chasma and associated CRISM spectra. a, RSL emanating from bedrock exposures at Coprates Chasma. Dark fans associated with RSL are indicated by arrows. Various coloured boxes show the approximate location of CRISM pixels shown in **b**. Section of HiRISE image ESP_031019_1650 ($L_S = 279°$, MY 31). **b**, Areas analysed in concurrent CRISM observation FRS00028E0A. Same RGB channels are used as in Fig. 1b. **c**, Spectra from the three coloured pixels in **b** are shown ratioed to nearby non-RSL material.

for the change in albedo of the fans, and may also explain spectral changes previously reported on RSL fans[4].

MRO's mid-afternoon (∼3 p.m.) observations occur at the time of the day with lowest relative humidity[19], which minimizes the probability of detecting liquid brines that emplaced hydrated salts, and may even facilitate dehydration of salts. In all sites discussed here, we observe H_2O-related absorption features at 1.9 and 3 μm, but the OH-related ∼1.4 μm feature is observed only in Palikir and Hale crater. On the basis of the widths and the band centres of the absorptions at 1.4 and 1.9 μm, a magnesium perchlorate, magnesium chlorate and magnesium chloride mixture was found to be the best match from our spectral mixture model (Supplementary Fig. 5). On the basis of spectral mixing models and absorption features at 2.15 and 2.43 μm, sodium perchlorate was found to be the best match at Horowitz (Fig. 2). We also performed similar spectral mixing models with various sulphates, but found no good match (Supplementary Fig. 6).

The presence of perchlorates on the surface of Mars has been confirmed at Gale crater by Mars Science Laboratory (MSL), the northern plains by the Phoenix mission, and is suspected at the Viking landing sites[6,20,21] (Supplementary Fig. 9). At Gale crater, hydrated calcium perchlorate is interpreted to be the best matching oxychlorine compound[6]. Magnesium perchlorate and calcium perchlorate were proposed as the most likely cation species of perchlorate at the Phoenix landing site[6,20,22]. Furthermore, thin films of water were suggested to have dissolved perchlorate from the surface to the subsurface and to have created concentrated patches at the Phoenix landing site[5,20]. Re-interpretation of the Viking data also found magnesium perchlorate to be the most likely perchlorate species[21]. These *in situ* perchlorate detections are consistent with our observation at RSL sites. Perchlorate and chlorate species have also been found in a Martian meteorite[23].

The origin of water forming the RSL is not understood[1–3]. Water could form by the surface/subsurface melting of ice, but the presence of near-surface ice at equatorial latitudes is highly unlikely[24]. RSL could form alternatively through deliquescence, but it is unclear whether the Martian atmosphere can supply sufficient water vapour every year to create RSL (ref. 2). Another hypothesis is seasonal discharge of a local aquifer, but lineae extending to the tops of local peaks[2] are difficult to explain. It is conceivable that RSL are forming in different parts of Mars through different formation mechanisms.

In all the sites reported here, we find evidence for hydrated salts on the RSL-containing slopes, supporting a genetic connection between the two. Sodium perchlorate can lower the freezing point of water by up to 40 K, whereas magnesium perchlorate and magnesium chlorate can depress the freezing point even more, by up to 70 K (refs 9,10,19). Magnesium chlorate, magnesium perchlorate and sodium perchlorate monohydrate are also predicted to be the most likely salts to concentrate from evaporation of brine at the Phoenix landing site[22]. Our observation of perchlorate could be due to liquid water in RSL dissolving perchlorates present in the soil and re-precipitating them in higher concentrations. Regardless, the spectral absorption of hydration bands at times and places when we observe maximum RSL activity implicates RSL as the source of hydrated salts.

These results strongly support the hypothesis that seasonal warm slopes are forming liquid water on contemporary Mars. The spectral identification of perchlorate in association with RSL also suggests that the water is briny rather than pure. Terrestrially, in the hyper-arid core of the Atacama Desert, deliquescence of hygroscopic salts offers the only known refuge for active microbial communities[25,26] and halophylic prokaryotes[27]. If RSL are indeed formed as a result of deliquescence of perchlorate salts, they might provide transiently wet conditions near surface on Mars, although the water activity in perchlorate solutions may be too low to support known terrestrial life[19]. The detection described here warrants further astrobiological characterization and exploration of these unique regions on Mars. This enhanced evidence for water flow also provides new clues as to the nature of the current Martian hydrologic cycle.

Methods

Methods and any associated references are available in the online version of the paper.

Received 22 April 2015; accepted 21 August 2015;
published online 28 September 2015; corrected online
14 October 2015

References

1. McEwen, A. S. *et al.* Seasonal flows on warm Martian slopes. *Science* **333,** 740–743 (2011).
2. McEwen, A. S. *et al.* Recurring slope lineae in equatorial regions of Mars. *Nature Geosci.* **7,** 53–58 (2014).
3. Ojha, L. *et al.* HiRISE observations of recurring slope lineae (RSL) during southern summer on Mars. *Icarus* **231,** 365–376 (2014).
4. Ojha, L. *et al.* Spectral constraints on the formation mechanism of recurring slope lineae. *Geophys. Res. Lett.* **40,** 5621–5626 (2013).
5. Hecht, M. H. *et al.* Detection of perchlorate and the soluble chemistry of martian soil at the Phoenix lander site. *Science* **325,** 64–67 (2009).
6. Glavin, D. P. *et al.* Evidence for perchlorates and the origin of chlorinated hydrocarbons detected by SAM at the Rocknest aeolian deposit in Gale Crater. *J. Geophys. Res.* **118,** 1955–1973 (2013).
7. Ehlmann, B. L. & Edwards, C. S. Mineralogy of the Martian surface. *Annu. Rev. Earth Planet. Sci.* **42,** 291–315 (2015).
8. Pestova, O. N., Myund, L. A., Khripun, M. K. & Prigaro, A. V. Polythermal study of the systems $M(ClO_4)_2$-H_2O ($M^{2+} = Mg^{2+}$, Ca^{2+}, Sr^{2+}, Ba^{2+}). *Russ. J. Appl. Chem.* **78,** 409–413 (2005).
9. Chevrier, V. F., Hanley, J. & Altheide, T. S. Stability of perchlorate hydrates and their liquid solutions at the Phoenix landing site, Mars. *Geophys. Res. Lett.* **36,** L10202 (2009).
10. Hanley, J., Chevrier, V. F., Berget, D. J. & Adams, R. D. Chlorate salts and solutions on Mars. *Geophys. Res. Lett.* **39,** L08201 (2012).
11. Altheide, T., Cheverier, V. F., Nicholson, C. & Denson, J. Experimental investigation of the stability and evaporation of sulfate and chloride brines on Mars. *Earth Planet. Sci. Lett.* **282,** 69–78 (2009).
12. Martín-Torres, F. J. *et al.* Transient liquid water and water activity at Gale crater on Mars. *Nature Geosci.* **8,** 357–361 (2015).
13. McEwen, A. S. *et al.* Mars Reconnaissance Orbiter's High Resolution Imaging Science Experiment (HiRISE). *J. Geophys. Res.* **112,** 1991–2012 (2007).
14. Murchie, S. *et al.* Compact Reconnaissance Imaging Spectrometer for Mars (CRISM) on Mars Reconnaissance Orbiter (MRO). *J. Geophys. Res.* **112,** 1–57 (2007).
15. Clark, R. N. in *Manual of Remote Sensing, Volume 3, Remote Sensing for the Earth Sciences* (ed. Rencz, A. N.) 3–58 (John Wiley, 1999).
16. Massé, M. *et al.* Spectroscopy and detectability of liquid brines on Mars. *Planet. Space Sci.* **92,** 136–149 (2014).
17. Hanley, J. *et al.* Reflectance spectra of hydrated chlorine salts: The effect of temperature with implications for Europa. *J. Geophys. Res.* **119,** 2370–2377 (2014).
18. Bishop, J. L., Quinn, R. & Darby, D. M. Spectral and thermal properties of perchlorate salts and implications for Mars. *Am. Mineral.* **99,** 1580–1592 (2014).
19. Rummel, J. D. *et al.* A new analysis of Mars "Special Regions": Findings of the Second MEPAG Special Regions Science Analysis Group (SR-SAG2). *Astrobiology* **14,** 887–968 (2014).
20. Cull, S. C. *et al.* Concentrated perchlorate at the Mars Phoenix landing site: Evidence for thin film liquid water on Mars. *Geophys. Res. Lett.* **37,** L22203 (2010).
21. Navarro-Gonzalez, R., Vargas, E., Rosa, J., Raga, A. C. & McKay, C. P. Reanalysis of the Viking results suggests perchlorate and organics at midlatitudes on Mars. *J. Geophys. Res.* **115,** E12010 (2010).
22. Elsenousy, A., Hanley, J. & Chevrier, V. F. Effect of evaporation and freezing on the salt paragenesis and habitability of brines at the Phoenix landing site. *Earth Planet. Sci. Lett.* **421,** 39–46 (2015).
23. Kounaves, S., Carrier, B. L., O'Neil, G. D., Stroble, S. T. & Claire, M. W. Evidence of Martian perchlorate, chlorate and nitrate in Mars meteorite EETA79001: Implications for oxidants and organics. *Icarus* **229,** 206–213 (2014).
24. Chevrier, V. F. & Rivera-Valentin, E. G. Formation of recurring slope lineae by liquid brines on present-day Mars. *Geophys. Res. Lett.* **39,** L21202 (2012).
25. Davila, A. F. *et al.* Facilitation of endolithic microbial survival in the hyperarid core of the Atacama Desert by mineral deliquescence. *J. Geophys. Res.* **113,** 2005–2012 (2008).
26. Davila, A. F., Hawes, I., Ascaso, C. & Wierzchos, J. Salt deliquescence drives photosynthesis in the hyperarid Atacama Desert. *Environ. Microbiol. Rep.* **5,** 583–587 (2013).
27. Aharon, O., Bardavid, R. E. & Mana, L. Perchlorate and halophilic prokaryotes: Implications for possible halophilic life on Mars. *Extremophiles* **18,** 75–80 (2014).
28. Hanley, J., Chevrier, V. F., Barrows, R. S., Swaffer, C. & Altheide, T. S. Near- and mid-infrared reflectance spectra of hydrated oxychlorine salts with implications for Mars. *J. Geophys. Res.* **120,** 1415–1426 (2015).
29. Crowley, J. K. Visible and near-infrared (0.4–2.5 μm) reflectance spectra of Playa evaporite minerals. *J. Geophys. Res.* **96,** 16231–16240 (1991).

Acknowledgements

L.O. and M.B.W. are funded by the National Science Foundation Graduate Research Fellowship Program under Grant No. DGE-1148903. The research was further supported by MDAP Grant No. NNX13AK01G. All original data described in this paper are reported in the SOM and archived by NASA's Planetary Data System. We thank the MRO science and engineering team for returning such an incredible data set. The paper benefited from initial reviews by B. Schmidt and L. Liuzzo.

Author contributions

The methodology was conceived and designed by L.O. All data analysis was done by L.O. with significant feedback from S.L.M., J.J.W., A.S.M. and M.B.W. J.J.W., M.B.W., J.H. and M.M. provided all the laboratory spectra used in this paper. A.S.M., M.C. and S.L.M. planned many of the HiRISE–CRISM coordinated observations of the RSL sites. All authors contributed to discussion, interpretation and writing.

Additional information

Supplementary information is available in the online version of the paper. Reprints and permissions information is available online at www.nature.com/reprints. Correspondence and requests for materials should be addressed to L.O.

Competing financial interests

The authors declare no competing financial interests.

Methods

Previous work[4] inspected only averages of many CRISM pixels, such that absorptions present over smaller areas would have been significantly weakened as a result of areal mixing. We extracted spectra from areas that had the widest RSL and normalized them using reference spectra from the same detector columns to avoid instrument artefacts (Supplementary Table 1). We also used multiple variants of the standard 'volcano-scan' approach to normalizing atmospheric absorptions to rule out inadvertent introduction of processing artefacts. Spectral mixing models used a spectrum from a spectrally neutral area within the same scene and column ('Martian soil'), combined with laboratory spectra of various salts, to find the best matching mixture of soil and a salt to the RSL spectra observed in CRISM data. A flow chart outlining how we separated signal from noise for the band detection algorithm routine is provided in Supplementary Fig. 10.

Organic compounds on comet 67P/Churyumov-Gerasimenko revealed by COSAC mass spectrometry

Fred Goesmann,[1*] Helmut Rosenbauer,[1] Jan Hendrik Bredehöft,[2] Michel Cabane,[3] Pascale Ehrenfreund,[4,5] Thomas Gautier,[6] Chaitanya Giri,[1,7] Harald Krüger,[1] Léna Le Roy,[8] Alexandra J. MacDermott,[9] Susan McKenna-Lawlor,[10] Uwe J. Meierhenrich,[7] Guillermo M. Muñoz Caro,[11] Francois Raulin,[12] Reinhard Roll,[1] Andrew Steele,[13] Harald Steininger,[1] Robert Sternberg,[12] Cyril Szopa,[3] Wolfram Thiemann,[2] Stephan Ulamec[14]

Comets harbor the most pristine material in our solar system in the form of ice, dust, silicates, and refractory organic material with some interstellar heritage. The evolved gas analyzer Cometary Sampling and Composition (COSAC) experiment aboard Rosetta's Philae lander was designed for in situ analysis of organic molecules on comet 67P/Churyumov-Gerasimenko. Twenty-five minutes after Philae's initial comet touchdown, the COSAC mass spectrometer took a spectrum in sniffing mode, which displayed a suite of 16 organic compounds, including many nitrogen-bearing species but no sulfur-bearing species, and four compounds—methyl isocyanate, acetone, propionaldehyde, and acetamide—that had not previously been reported in comets.

The study of the chemical composition of comets provides key information about the raw materials present in the early solar system (*1*, *2*). Ground and space-based observations have identified over 20 organic molecules in comet comae (*3*, *4*), a subset of which are of prebiotic interest (*5*, *6*).

The Cometary Sampling and Composition (COSAC) experiment on Rosetta's lander Philae was designed to detect and identify organic molecules in the material of comet 67P (*7*). It consists of a gas chromatograph (GC) and a time-of-flight mass spectrometer (TOF-MS) to analyze samples delivered by the sample drilling and distribution system (SD2). COSAC can also operate in sniffing mode, in which the MS accumulates data without active sampling by SD2. Molecules that have passively entered the instrument are ionized, accelerated, and finally registered by COSAC. MS sniffings were made several times between launch and arrival at the comet, including during a fly-by of Lutetia (*8*). MS sniffings were made on arrival at 67P from 10 km above the surface, after initial touchdown, and at the final resting site (Fig. 1).

The Philae lander first touched down on 67P on 12 November 2014 at 15:34:04 UTC and then bounced. The impact excavated about 0.4 m^3 of solid material (*9*), some of which would have entered COSAC's two exhaust pipes, which are on the bottom of the lander (*10*), and then stuck to the inside of the 2-cm-wide pipes. The temperature in these pipes was 12° to 15°C (*10*), midway between the cold cometary exterior and the heated interior of the lander, allowing volatile organics to sublime and be detected by the MS in a measurement that began at 16:00:30 UTC and ended at 16:02:50 UTC, when the lander was about 150 m above the surface on its first bounce. We focus here on this spectrum (green in Fig. 1), which differs fundamentally in the number and intensity of its peaks from the undisturbed spectra taken before and after, and represents excavated cometary material (*10*). Our approach was to find the best fit to this spectrum of a superposition of standard National Institute of Standards and Technology (NIST) mass spectra (*11*) of candidate cometary molecules. The spectral deconvolution methodology used is similar to that used in other space missions [such as the Ion and Neutral Mass Spectrometer (INMS) measurements by Cassini and the GCMS on the Huygens probe] (*12*–*14*).

Because COSAC has a mass resolution of only 300, single mass peaks cannot be resolved into different molecular species [e.g., CO, N_2, and C_2H_4, all at a mass/charge ratio (m/z) of 28, are indistinguishable]. Analysis (*10*) was limited to compounds below m/z 62 because signals beyond this value are too faint to be distinguished reliably from noise. The peak at m/z 78, for example, is not real: Several ions coincidentally ended up in a single channel, leaving neighboring ones empty (*10*). All conceivable molecules were first listed and their fragmentation patterns evaluated (table S1). Elimination of molecules with incompatible fragmentation patterns (for reasons described in table S3) led to a short-list of candidate molecules (table S2). We further reduced the short list by making the fit in order of decreasing mass,

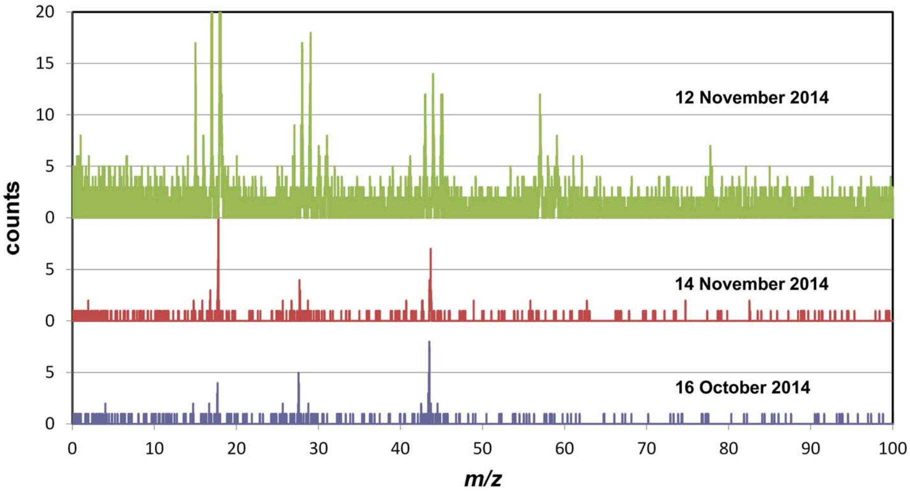

Fig. 1. Mass spectra taken by COSAC in "sniffing mode." Top (green): spectrum taken 25 min after first touchdown; the m/z 18 peak reached a height of 330 counts, but the spectrum is truncated to show smaller peaks more clearly; middle (red): final spectrum, taken 2 days later at the current Philae position; bottom (blue): first spectrum, obtained in orbit 27 days before landing, from a distance of 10 km.

---

[1]Max Planck Institute for Solar System Research, Justus von Liebig Weg 3, 37077 Göttingen, Germany. [2]University of Bremen, Institute for Applied and Physical Chemistry, Leobener Strasse NW2, 28359 Bremen, Germany. [3]Université Versailles St-Quentin, Sorbonne Universités, Université Pierre et Marie Curie Univ. Paris 06, Centre National de la Recherche Scientifique (CNRS)–Institut National des Sciences de l'Univers, Laboratoire Atmosphéres, Milieux, Observations Spatiales–Institut Pierre Simon Laplace (LATMOS-IPSL), 4 Place Jussieu 75005 Paris. [4]Leiden Observatory, Post Office Box 9513, 2300 RA Leiden, Netherlands. [5]Space Policy Institute, George Washington University, Washington, DC, USA. [6]Goddard Space Flight Center, Greenbelt, MD 20771, USA. [7]University Nice Sophia Antipolis, Institut de Chimie de Nice Unite Mixte de Recherche (UMR) 7272 CNRS, Avenue Valrose, 06108 Nice, France. [8]Center for Space and Habitability, University of Bern, Sidlerstrasse 5, CH-3012 Bern, Switzerland. [9]University of Houston–Clear Lake, 2700 Bay Area Boulevard, Houston, TX 77058, USA. [10]Space Technology Ireland, Ltd., Maynooth, Co. Kildare, Ireland. [11]Centro de Astrobiología, Instituto Nacional de Técnica Aeroespacial–Consejo Superior de Investigaciones Científicas, Ctra. de Ajalvir, km 4, Torrejón de Ardoz, 28850 Madrid, Spain. [12]Laboratoire Interuniversitaire des Systèmes Atmosphériques (LISA), UMR CNRS 7583, Université Paris-Est Créteil and Université Paris-Diderot, 94000 Créteil, France. [13]Geophysical Laboratory, Carnegie Institution of Washington, Washington, DC, USA. [14]German Aerospace Center, Deutsches Zentrum für Luft und Raumfahrt (DLR), 51147 Cologne, Germany.
***Corresponding author. E-mail: goesmann@mps.mpg.de**

starting from *m/z* 59 (*10*), and eliminating unstable and unsaturated species. This yielded a good fit to all peaks (except *m/z* 15 and a fraction of *m/z* 29, Fig. 2) with 16 species from several families of molecules—alcohols, carbonyls, amines, nitriles, amides, and isocyanates—in a consistent combination (Table 1). Peaks for *m/z* < 10 were not included in the fit because they are not listed in the standard NIST mass spectra (*11*). The molecular abundances of these compounds relative to that of water (Table 1) were corrected for electron cross section (table S4). The absence of ions at *m/z* 32 indicates a lack of sulfur-bearing species (Fig. 2 and Table 1). Amino acids were not included in the fit because the molecular ion peaks of glycine (*m/z* 75) and alanine (*m/z* 89) are negative after background subtraction, thereby suggesting that they are noise. Although fragment peaks assigned to glycine and alanine in the NIST standard spectra (*11*) are present in the COSAC spectrum (in the *m/z* 30s to 40s range), any contribution to these fragment peaks from amino acids is difficult to disentangle from the contributions of other species.

The main source of error is the low signal intensity, averaging about 100 counts (table S1). A statistical square-root of *n* approach yields a standard deviation of 10%. In addition, the NIST standard spectra (*11*) have a 15% error. Considering formal error propagation and the uncertainties in our peak-fitting algorithm, we estimate that the abundances given in Table 1 are accurate to about a factor of 2. The fit of a mass spectrum whose peaks result from the superposition of different molecular species is intrinsically degenerate, with several possible solutions (*10*).

The absence of large quantities of NH_3, HCHO, and CO_2 in our best fit may seem surprising because they were expected to be present as components of cometary ice. NH_3 (*m/z* 17) was not needed for the fit, but the presence of small quantities seems likely. However, this is hard to quantify because the large H_2O peak at *m/z* 18 implies a substantial contribution to the *m/z* 17 peak from the OH fragment peak of H_2O, which is difficult to distinguish from any NH_3 contribution. HCHO (*m/z* 30) and CO_2 (*m/z* 44) are not included because *m/z* 30 is mainly accounted for by fragment peaks of other molecules, rather than by the molecular ion of HCHO, and *m/z* 44 is mainly accounted for by fragment contributions from acetamide, formamide, and acetaldehyde, rather than by CO_2.

We initially tried a fit that started with the assumption that *m/z* 44 came from CO_2, but no acceptable fit could be achieved to the remaining peaks. If all of *m/z* 44 were ascribed to CO_2, our sample would only contain 3% of CO_2 relative to water. Using the procedure described above, we found that a more sensible fit for all mass peaks, especially *m/z* 57, 58, and 59, could only be achieved by assuming a CO_2 concentration of less than 0.1%. The low abundance of CO_2, NH_3, and HCHO could indicate that the excavated COSAC sample came from an area depleted in volatile ice components. Observations by the Visible, Infrared and Thermal Imaging Spectrometer (VIRTIS) from the Rosetta orbiter (*15*) do suggest a dark surface depleted in volatiles, consisting mainly of refractory organic macromolecular materials, with very little ice on the surface. Studies (*16*) using the Rosetta Orbiter Spectrometer for Ion and Neutral Analysis (ROSINA) indicate that volatile ices sublime diurnally and seasonally, with CO_2 ranging from 3% relative to water in local summer (the present case) to 80% in local winter.

The COSAC findings differ from those of Ptolemy (*17*) because COSAC sampled particles excavated by the impact (*10*) that entered the warm

Fig. 2. The fit to the observed spectrum. Comparison of the COSAC original mass spectrum (black bars for each integer mass) and the spectrum reconstructed from the best fit (orange bars to right of original signal). The peak heights are normalized to 100 for the *m/z* 18 peak (which has been truncated).

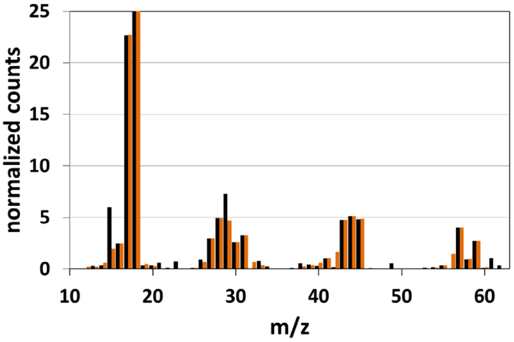

Table 1. The 16 molecules used to fit the COSAC mass spectrum.

Name	Formula	Molar mass (u)	MS fraction	Relative to water
Water	H_2O	18	80.92	100
Methane	CH_4	16	0.70	0.5
Methanenitrile (hydrogen cyanide)	HCN	27	1.06	0.9
Carbon monoxide	CO	28	1.09	1.2
Methylamine	CH_3NH_2	31	1.19	0.6
Ethanenitrile (acetonitrile)	CH_3CN	41	0.55	0.3
Isocyanic acid	HNCO	43	0.47	0.3
Ethanal (acetaldehyde)	CH_3CHO	44	1.01	0.5
Methanamide (formamide)	$HCONH_2$	45	3.73	1.8
Ethylamine	$C_2H_5NH_2$	45	0.72	0.3
Isocyanomethane (methyl isocyanate)	CH_3NCO	57	3.13	1.3
Propanone (acetone)	CH_3COCH_3	58	1.02	0.3
Propanal (propionaldehyde)	C_2H_5CHO	58	0.44	0.1
Ethanamide (acetamide)	CH_3CONH_2	59	2.20	0.7
2-Hydroxyethanal (glycolaldehyde)	CH_2OHCHO	60	0.98	0.4
1,2-Ethanediol (ethylene glycol)	$CH_2(OH)CH_2(OH)$	62	0.79	0.2

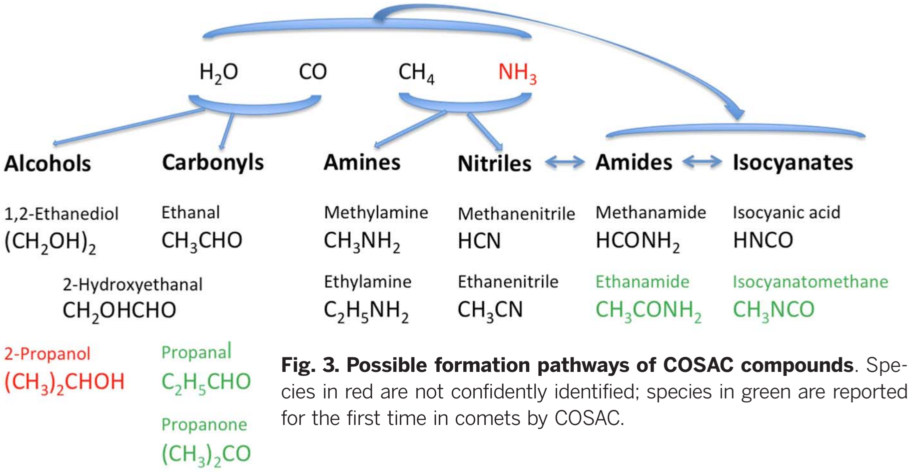

Fig. 3. Possible formation pathways of COSAC compounds. Species in red are not confidently identified; species in green are reported for the first time in comets by COSAC.

exhaust tubes located on the bottom of the lander, where they pointed toward the surface, whereas Ptolemy sampled ambient coma gases entering exhaust tubes located on top of the lander, where they pointed toward the sky (possibly with the addition of some dust that made its way around the lander). That COSAC detected far more nitrogen-bearing compounds than Ptolemy agrees with earlier observations that nitrogen was more abundant in the dust than in the gas of comet Halley (*18*). The Ptolemy team interpret their mass spectrum as fragments of polyoxymethylene polymer, with a strong CO_2 peak of intensity 20% relative to water. COSAC did not detect ambient coma gases (which were dominated in Ptolemy data by CO_2 with a few polymer fragments). The COSAC MS maintains a constant pressure; thus, subliming gases from our ground sample pushed the ambient coma gases outside the COSAC MS. Before sublimation, the total pressure inside the COSAC MS was dominated by CO_2, in line with Ptolemy data and prelanding COSAC spectra. After sublimation, the total pressure inside the COSAC MS was due to the sum of the partial pressures of all the sublimed ground materials. This can explain the missing CO_2 in the post-touchdown spectrum. The displacement of ambient coma gases by subliming ground materials and the temperature of 12° to 15°C in the COSAC exhaust tubes, which is too low to break down any refractory polymers in the ground materials, combine to explain why COSAC did not detect any polymer fragments.

The COSAC molecules form a consistent set related by plausible formation pathways (Fig. 3). A nitrogen source such as NH_3 must originally have been abundant to form the many N-bearing species, but could since have mostly evaporated or been used up in reactions. All the COSAC organics can be formed by UV irradiation and/or radiolysis of ices due to the incidence of galactic and solar cosmic rays: alcohols and carbonyls derived from CO and H_2O ices (*19*), and amines and nitriles from CH_4 and NH_3 ices (*20*). Hydrolysis of nitriles produces amides, which are linked to isocyanates by isomerization.

Several of the COSAC compounds, such as HCN, CH_3CN, and HNCO, are present in the comae of most comets (*1*). Others, such as CH_3CHO, $HCONH_2$, $CH_2(OH)CH_2(OH)$, CH_3NH_2, and $C_2H_5NH_2$, have only been found in a few comets. Four molecules reported by COSAC—CH_3NCO, CH_3COCH_3, C_2H_5CHO, and CH_3CONH_2—have not been previously reported in a cometary environment, and CH_2OHCHO has only been reported as an upper limit. These cometary molecules are all predicted by our generalized formation scheme (Fig. 3). CH_2OHCHO is an efficient initiator in the prebiotic formation of sugars (*21*). HCN is a key molecule in the prebiotic synthesis of amino acids (*21*, *22*) and nucleobases (*21*) and even offers an elegant pathway to sugars (*23*). $HCONH_2$ provides a prebiotic route to nucleobases (*24*). $HCONH_2$ (*24*) and CH_3CONH_2 (*21*) catalyze phosphorylation of nucleosides to nucleotides, in which amines also play a role (*21*). Isocyanates play a major role in the prebiotic synthesis of peptides, through the so-called isocyanate route (*22*). The complexity of cometary nucleus chemistry and the importance of N-containing organics imply that early solar system chemistry fosters the formation of prebiotic material in noticeable concentrations.

REFERENCES AND NOTES

1. M. J. Mumma, S. B. Charnley, The chemical composition of comets—emerging taxonomies and natal heritage. *Annu. Rev. Astron. Astrophys.* **49**, 471–524 (2011). doi: 10.1146/annurev-astro-081309-130811
2. J. Greenberg, *Astron. Astrophys.* **330**, 375–380 (1998).
3. J. Crovisier *et al*., The chemical diversity of comets: Synergies between space exploration and ground-based radio observations. *Earth Moon Planets* **105**, 267–272 (2009). doi: 10.1007/s11038-009-9293-z
4. M. DiSanti, M. Mumma, Reservoirs for comets: Compositional differences based on infrared observations. *Space Sciences Series* **28**, 127–145 (2008). doi: 10.1007/978-0-387-85455-7_8
5. J. Oró, T. Mills, A. Lazcano, Comets and the formation of biochemical compounds on the primitive Earth—a review. *Orig. Life Evol. Biosph.* **21**, 267–277 (1992). doi: 10.1007/BF01808302; pmid: 11537542
6. W. M. Irvine, Extraterrestrial organic matter: A review. *Orig. Life Evol. Biosph.* **28**, 365–383 (1998). doi: 10.1023/A:1006574110907; pmid: 9742722
7. F. Goesmann *et al*., Cosac, The cometary sampling and composition experiment on Philae. *Space Sci. Rev.* **128**, 257–280 (2007). doi: 10.1007/s11214-006-9000-6
8. F. Goesmann *et al*., Interpretation of COSAC mass spectrometer data acquired during Rosetta's Lutetia fly-by 10 July 2010. *Planet. Space Sci.* **66**, 187–191 (2012). doi: 10.1016/j.pss.2012.01.012
9. J. Biele *et al*., The landing(s) of Philae and inferences on comet surface mechanical properties. *Science* **349**, aaa9816 (2015).
10. Full details and methods are in the supplementary materials on *Science* Online.
11. S. E. Stein, in *NIST Chemistry WebBook*, NIST Standard Reference Database Number 69, P. J. Linstrom, W. G. Mallard, Eds. (National Institute of Standards and Technology, Gaithersburg, MD); http://webbook.nist.gov.
12. J. H. Waite Jr. *et al*., Ion neutral mass spectrometer results from the first flyby of Titan. *Science* **308**, 982–986 (2005). doi: 10.1126/science.1110652; pmid: 15890873
13. K. E. Mandt *et al*., Ion densities and composition of Titan's upper atmosphere derived from the Cassini Ion Neutral Mass Spectrometer: Analysis methods and comparison of measured ion densities to photochemical model simulations. *J. Geophys. Res. Solid Earth* **117** (E10), E10006 (2012). doi: 10.1029/2012JE004139
14. J. H. Waite Jr. *et al*., Cassini ion and neutral mass spectrometer: Enceladus plume composition and structure. *Science* **311**, 1419–1422 (2006). doi: 10.1126/science.1121290; pmid: 16527970
15. F. Capaccioni *et al*., Cometary science. The organic-rich surface of comet 67P/Churyumov-Gerasimenko as seen by VIRTIS/Rosetta. *Science* **347**, aaa0628 (2015). pmid: 25613895
16. M. Hässig *et al*., Time variability and heterogeneity in the coma of 67P/Churyumov-Gerasimenko. *Science* **347**, aaa0276 (2015). doi: 10.1126/science.aaa0276; pmid: 25613892
17. I. P. Wright *et al*., CHO-bearing organic compounds at the surface of 67PChuryumov-Gerasimenko revealed by Ptolemy. *Science* **349**, aab0673 (2015).
18. S. Wyckoff, S. C. Tegler, L. Engel, Nitrogen abundance in Comet Halley. *Astrophys. J.* **367**, 641–648 (1991). doi: 10.1086/169659
19. G. M. Muñoz Caro, E. Dartois, Prebiotic chemistry in icy grain mantles in space. An experimental and observational approach. *Chem. Soc. Rev.* **42**, 2173–2185 (2013). doi: 10.1039/c2cs35425j; pmid: 23340705
20. Y. S. Kim, R. I. Kaiser, on the formation of amines (RNH_2) and the cyanide anion (CN^-) in electron-irradiated ammonia-hydrocarbon interstellar model ices. *Astrophys. J.* **729**, 68–75 (2011). doi: 10.1088/0004-637X/729/1/68
21. L. E. Orgel, Prebiotic chemistry and the origin of the RNA world. *Crit. Rev. Biochem. Mol. Biol.* **39**, 99–123 (2004). doi: 10.1080/10409230490460765; pmid: 15217990
22. R. Pascal, L. Boiteau, A. Commeyras, From the prebiotic synthesis of α-amino acids towards a primitive translation apparatus for the synthesis of peptides. *Top. Curr. Chem.* **259**, 69–122 (2005). doi: 10.1007/b136707
23. D. Ritson, J. D. Sutherland, Prebiotic synthesis of simple sugars by photoredox systems chemistry. *Nat. Chem.* **4**, 895–899 (2012). doi: 10.1038/nchem.1467; pmid: 23089863
24. R. Saladino, C. Crestini, F. Ciciriello, G. Costanzo, E. Di Mauro, Formamide chemistry and the origin of informational polymers. *Chem. Biodivers.* **4**, 694–720 (2007). doi: 10.1002/cbdv.200790059; pmid: 17443884

ACKNOWLEDGMENTS

This work was supported by Deutsches Zentrum für Luft- und Raumfahrt (DLR) under contract no. 50 QP 1302, and by Centre National d'Etudes Spatiales (CNES) grants at LATMOS and LISA. U.J.M. was funded by L'Agence Nationale de la Recherche (ANR-12-IS07-0006). Support from the NASA Astrobiology Institute (P.E.), the NASA Postdoctoral Program at Goddard Space Flight Center (T.G.), Programme de Développement d'Expériences scientifiques through Enterprise Ireland (S.McK.L.), and the Welch Foundation (A.J.MacD.) is acknowledged. Rosetta is a European Space Agency (ESA) mission with contributions from member states and NASA. The Philae lander was provided by a consortium led by DLR, Max-Planck-Institut für Sonnensystemforschung, CNES, and Agenzia Spatiale Italiana. The data used in this study are available through ESA's Planetary Science Archive (www.rssd.esa.int/index.php?project=PSA&page=rosetta).

SUPPLEMENTARY MATERIALS

www.sciencemag.org/content/349/6247/aab0689/suppl/DC1
Materials and Methods
Figs. S1 and S2
Tables S1 to S4
References (*25*–*32*)

9 March 2015; accepted 1 July 2015
10.1126/science.aab0689